Influence of joining technique on electromagnetic properties and corrosion behaviour of dissimilar weld joints

Veeraiah G[1,2*], Ramanaiah N[2], Sudhakar I[1], B Srinivas[1]

[1]Department of Mechanical Engineering, MVGR College of Engineering (A), Vizianagaram, 535005, India
[2]Department of Mechanical Engineering, AU college of Engineering, Andhra University, Visakhapatnam, India
Corresponding should be addressed to Veeraiah G, Email: veeraiah@mvgrce.edu.in, veerumech307@gmail.com

Abstract

Welding is one of the greatest and most suitable procedures for producing complicated things for aerospace, naval, and automotive components. Due to service needs and the complexity of load acting, manufacturing organisations are forced to blend materials of various types. Effective welding techniques are therefore necessary, as is understanding of flaws and their repercussions. In this study, the viability of combining two dissimilar aluminium alloys has been investigated utilising two distinct welding processes: friction stir welding (FSW) and TIG welding. The two aluminium alloys AA5083-O and AA7075-T651 were successfully welded together using weld currents (80-120 amp for TIG and 800, 1000, 1100, 1200, and 1400 rpm with constant traverse speed for FSW). An attempt has been made to study the effect of joining technique on EM wave properties of dissimilar aluminium alloy joints. Further, TIG welded joints were characterized for pitting corrosion behaviour.

Keywords: Fusion and Solid state welding techniques, weld current, TRS (tool rotational speed), EM wave properties and corrosion

1.0 Introduction

Modern aircraft and navy ships replace mechanical, hydraulic, pneumatic, and electromechanical systems with electronic components. The likelihood of electromagnetic interference (EMI)-related device malfunctions increasing sharply with increased use of electronic devices [1-2]. When radar and lightning strikes produce high intensity electromagnetic fields, EMI arises when an electronic system is subjected to them. The three main modes of electromagnetic shielding are reflection (R), multiple reflection (M), and absorption (A). Remaining energy after reflection is referred to as residual energy, and the ratio of residual to disturb energy is known as shielding efficacy (SE). The presence of electrons or holes (charge carriers) in the material or shield is necessary for efficient electromagnetic wave interaction [3-4]. The ability of warships or aircraft to be detected by an adversary's radar signals determines their capacity to survive in a hostile environment. There are generally two ways to increase the efficiency of the shielding. One is body form optimization, which causes the produced electromagnetic wave to scatter and produce the least amount of reflection. Body shape optimization, however, affects the design and has a further impact on aerodynamic performance. The other is using materials that absorb electromagnetic waves to lessen these issues [5]. As a result, materials that absorb radar, such as polymer reinforced composites and composites with conductive fillers like carbon fibres or

particles, metal fibres or flakes, are in high demand. In comparison to metals and alloys, polymer composites' principal disadvantages are their extremely low strength, weak mechanical characteristics, and environmental resistance. Additionally, they need ongoing maintenance and are unsuitable for structures that support loads [6]. As a result, traditional materials like steel, nickel, and permalloy must be employed for EMI shielding. However, due to their high density, their use is constrained. Instead, researchers are concentrating on low dense materials such aluminium composites and the production of metal foams for EMI applications. Additionally, in fields like shipbuilding and aerospace, these materials can be successfully utilised as load-bearing structures. The use of metal matrix composites and aluminium alloys as EMI shields has received very little attention. The EMI and mechanical properties of the hybrid composite are better than those of the substrate in the aluminium alloy reinforced with fly ash, Al2O3, and SiC, and the efficiency of the shielding is related to the percentage of reinforcement [7-8]. In the frequency range of 30 KHz to 1.5 GHz, Do Z et al. examined the shielding efficiency of aluminium metal matrix composites. In the 30 KHz to 600 MHz frequency band, EMI shielding efficiency increased. Additionally, when frequency increased, composites' shielding efficiency increased [9]. A unique sandwich composite constructed of ferro-aluminum for shielding magnetic and electromagnetic interference was produced by hot pressing and subsequent diffusion treatment. The electromagnetic shielding effectiveness of sandwich composite is higher than that of a pure iron plate and increases with diffusion period length, reaching 70 to 80 dB at frequencies between 30 KHz and 1.5 GHz. The multiple reflection loss in the Fe-Al gradient layer is a crucial component in enhancing the shielding performance of sandwich composite [2]. The electromagnetic interference shielding efficacy (EMSE) properties of the composites were assessed in the frequency range of 30.0 kHz-1.5 GHz. The results demonstrated that the EMSE characteristics of the two different types of composites were essentially equivalent. The addition of fly ash particles improved the shielding efficiency properties of the matrix aluminium in the frequency ranges of 30.0 kHz–600.0 MHz, and the increment varied with rising frequency [10]. Significant changes have been made to the shielding effectiveness of aluminium 6061 composite strengthened with al2o3, SiC, and fly ash. Excellent mechanical and EM shielding characteristics were demonstrated by composites made with 10 weight percent of Al2O3 and SiC and 5 weight percent of fly ash [8]. Similar findings on Al6061 composites reinforced with the aforementioned elements were discovered [1]. The electromagnetic shielding efficacy of cement-based materials is significantly decreased by the inclusion of nickel fibre. With more nickel fibres present, the SE of the nanocomposites using cement as the base directly rises. At 120 MHz, a composite made with doped nickel fibre had the highest recorded shielding efficacy, which was 24.48 dB [11]. Despite challenges with joining, researchers were able to create successful EM shielding materials using aluminium alloy and composites. Due to their weak joining capabilities, the use of aluminium alloys and composites is restricted to certain applications. Numerous researchers looked into how the TIG welding process affected the mechanical characteristics of aluminium alloys. TIG welding was used to evaluate the joining of AA5083 aluminium alloy in order to determine the ideal processing variables, such as weld current and gas flow rate, for increased bond strength. It was found that joining aluminium alloys did not benefit from high heat intake or high current [12]. Joints with no defects were produced when fusing AA5456 with argon as the shielding gas. During pulse TIG welding of an aluminium alloy, peak current, base current, welding speed, and pulse frequency all had an impact on creating a thin, equiaxed

grain structure in the weld zone [13]. Cold metal transfer (CMT), TIG, and TIG-CMT hybrid welding techniques were used to weld AA 6061 aluminium alloy. Results of the comparison showed that the hybrid joint's weld penetration was deeper than the sum of the penetrations of the TIG joint and the CMT weld joint [14]. TIG welding was used to join two distinct aluminium alloys, AA2024-T3 and AA7075-T6, utilising two tungsten electrodes. The use of twin electrodes, the researchers found, produced an arc that was stable and had excellent weld bead appearance. The weld zone micro hardness is lower than HAZ on the AA7075 alloy side. Maximum weld joint tensile strength is inferior to the strengths of base alloys AA7075-T6 and AA2024-T3 by 44% and 37%, respectively [15]. Friction stir welding (FSW), a new method that was patented by the UK's Welding Institute in 1991, seems to be a workable replacement for conventional welding techniques because it is less expensive, lighter, uses less energy, emits fewer greenhouse gases, and has better metallurgical properties [16]. FSW is an autonomous, continuous hot shearing process that is used to join materials while their solidus temperatures are below them. A non-consumable rotating tool that is tougher than the materials being joined enters the plates' abutting edges and moves along the joint line during welding. The base material is placed so that the retreating side (RS) faces away from the tool velocity vector and the advancing side (AS) faces the tool velocity vector. (RS). The non-consumable tool is made up of two different parts: the shoulder and a pin with a specific profile. The contact heat produced by rotating tools results in significant plastic deformation of base materials. The tool extrudes the weaker material [16-19]. Two distinct aluminium alloys, AA5754-H111 and AA7075-T651, were joined using the FSW technique. A defect-free joint with a maximum tensile strength of 239 MPa is produced when the tool traverse and rotational speeds are 80 mm/min and 1000 rpm, respectively [20]. Two distinct aluminium alloys, AA5383 and AA7075, were successfully joined by friction stir welding (FSW). A tool rotating speed of 700 rpm and a traverse speed of 40 mm/min were used to achieve a weld joint tensile strength of 211 Mpa [21]. Corrosion behaviour of friction stir weldedAA6061-T3 alloy was investigated by Waseem et al., (2021). Two distinct rotational speeds (850 and 950 rpm) and a constant travel speed (22 mm/min) were used for the FSW. The effects of two tool pin profiles straight cylindrical and conical on corrosion protection were investigated. According to the findings, the welded alloy has less corrosion protection than BM. In both NaCl and KCl media, lower rotational speed (850 rpm) led to welds with greater corrosion protection. In both NaCl and KCl media, the conical tool pin profile produced weld with greater corrosion resistance than the straight cylinder pin. NaCl observed a nearly two-fold increase in corrosion rate [22]. Corrosion Behaviour of Friction Stir Welded AA8090-T87 Aluminum Alloy was studied by chandrasekharan et.al. Tool rotational speed of 900 rpm and traverse speeds of 90 mm/min., 110 mm/min are the considered welding parameters. The analysis suggests that the change in tool traverse speed transformed the corrosion behaviour of the joint and affected both the hardness and surface roughness which mitigated the quality of the joint [23]. The change in corrosion susceptibility between several friction stir-welded, AA5456 thick plate sections was examined by Fonda et al. They discovered that the nugget region, which has a large concentration of β precipitates, is where the corrosion attack was primarily seen [24]. Aluminium alloys are welded successfully through TIG and FSW processes. However, researchers mainly concentrated on mechanical characterization and there is a vacuum to study the effect of joining technique on EM wave properties of the welded joints. In the present investigation authors made an attempt to study

the effect of TIG and FSW techniques on EM wave properties of dissimilar AA5083-O and AA7075-T651 aluminium alloy joints fabricated through aforementioned weld techniques.

2.0 Materials and Methods

Base materials were purchased from perfect metal works Bangalore, India. Spectroscopy method used to identify the chemical composition of the base materials and the corresponding results presented in table-1.

Table 1: Chemical composition of base alloys and electrode used in TIG

Base alloys & Electrode	Element (in wt. %)								
	Si	**Fe**	**Cu**	**Mn**	**Mg**	**Cr**	**Zn**	**Ti**	**Aluminum**
AA7075-T651	0.04	0.15	1.3	0.02	2.3	0.19	5.4	0.05	Balance
AA5083-O	0.09	0.27	0.01	0.8	4.4	0.07	0.02	0.02	Balance
ER5083	0.09	0.27	0.01	0.8	4.4	0.07	0.02	0.02	Balance

100*75*3-sized pieces of the basic alloys AA5083-O and AA7075-T651 are cut from rolled sheets using a water jet cutting technique. TIG welding is done using the EWM 500 Tetrix 500 AC/DC equipment at five different weld currents. (80 amp-120 amp). Using an NC FSW machine (Make: R.V. Machine tools, Coimbatore) base metals are friction stir welded. Tool with rotational speeds of 800, 1000, 1100, 1200, and 1400 rpm and a constant traverse speed of 40 mm/min were utilised to fabricate weld joints. A software-based Gill AC electrochemical system was utilised to carry out potentio dynamic polarisation tests in accordance with ASTM G106 standard in order to evaluate the pitting corrosion behaviour. All tests were carried out in solutions containing 3.5% NaCl that had their pH raised to 10 by the addition of potassium hydroxide. Using a vector network analyzer (Rhodes & Schwarz model ZVB 20) through waveguide technology, all the manufactured weld joints were characterised for EM wave properties as permeability, permittivity, conductivity, and shielding efficacy in the X-band frequency (8.2-12.4 GHz).

3.0 Results and Discussion

3.1 EM shielding characteristics of TIG welded joints

The expansion of electronic devices has led to an increase in electromagnetic interference. Electrostatic discharge is a significant cause of EMI. The signal radiations that EMI produces have the potential to seriously damage electronic devices. An electromagnetic pulse consists mainly of two perpendicular fields, one each for the magnetic and electric. Forces are produced on the charge carriers as a result of the electric field's influence [25]. When the conductor's ideal surface makes contact with the electric field, the current will be induced. As a result, the conductor experiences charge displacement, further cancelling the supplied electric field and stopping the current. The generated changing magnetic field cancels out the applied magnetic field in a similar way. The effectiveness of base alloys and weld joints for EMI shielding is assessed using a two port vector network analyzer. On the surface, oblique electromagnetic impulses regularly impinge. However, because to the limits of the VNA via

waveguide technology, the incidence angle examined in the current study is 90° [1, 5, 8]. Using the EM wave theory, the EMI SE of the two basic alloys and the produced weld joints are measured. The following equation is used to determine the electromagnetic shielding effectiveness (Reflection power, Absorption power, and Transmission power) in terms of S parameters [8].

$$SE_T = 10 \log 10\frac{1}{T} = 10 \log 10\frac{1}{|S12|2} = 10 \log 10 \frac{1}{|S21|2}$$

There are two different sorts of currents in the electric field that are present when an EMI incidents on a metallic surface. (Conduction and displacement). The displacement current and the conductance current are two real and one hypothetical components of permittivity.

Fig. & the complex permittivity and permeability of TIG weld joints created with varied weld currents are shown. Permittivity of weld joints increases with weld current and is almost constant independent of frequency. It may be seen because as the weld current rises, the conductive network is rapidly expanding and forming pores. When EM radiation strikes metallic surfaces, it creates an electric field that causes two different types of electrical currents to flow through the material. They are the displacement current produced by bound charges and the conduction current produced by unbound electrons in the metal. Conduction current will contribute to the imaginary part of the permittivity, whereas displacement current will contribute to the real portion. (dielectric loss).

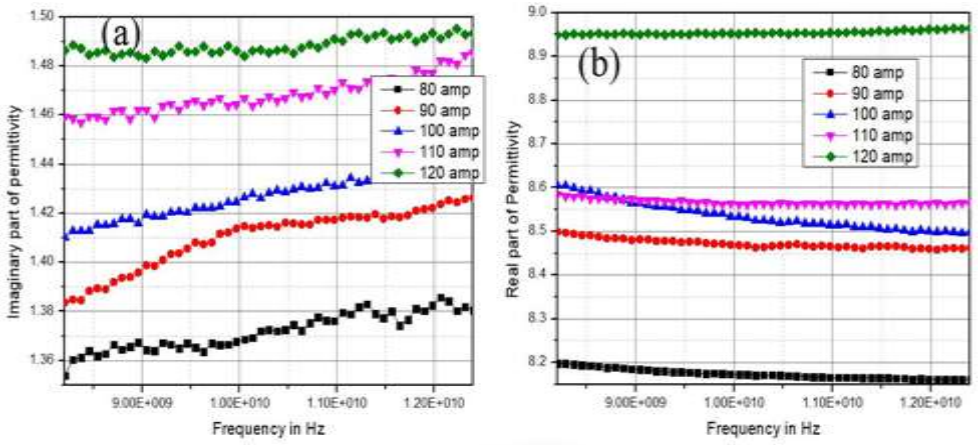

Fig.1 Permittivity of TIG weld joints

The real component of permeability has a range of 1.08 to 1.23 and the imagined component has a range of -0.7 to -1.1. The low weld joint permeability values imply that a significant portion of the weld joints' microwave absorption is caused by dielectric loss. Real permeability is higher than imaginary permeability in the X-band frequency range (Real permeability = 1, Imaginary permeability = 0), and real permeability rises with joint currents, as seen in Figure.2 The SE of weld joints varies in the 8.2 GHz to 12.4 GHz frequency range. Additionally, all weld joints show a consistent pattern, with their SE falling between -8.1 dB and -10.5 dB.

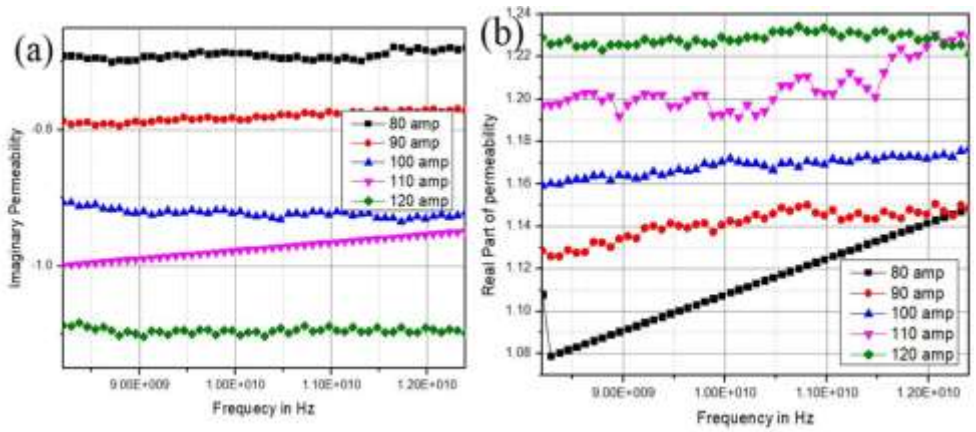

Fig.2 Permeability of TIG weld joints

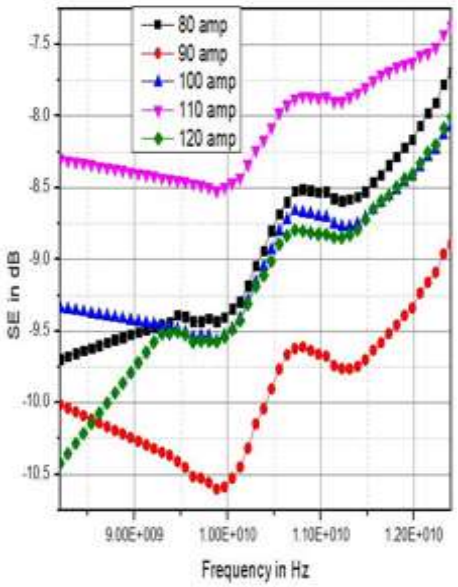

Fig.3 shielding effectiveness of TIG weld joints

3.2 EM shielding characteristics of FSW joints

The components of complex permittivity and permeability of base alloys and FSW weld joints are depicted in Figures 4 and 5 as both imaginary and real, respectively. Base alloys have a lower permittivity than weld joints, and for weld joints, it increases with increasing tool rotational speed. However, regardless of the rate of tool rotation, the permittivity of weld joints remains constant over the whole frequency range. The rise in permittivity of weld joints may be caused by the development of porosity and the accumulation of conductive networks as a result of the production of voids with an increase in tool rotating speed [26].

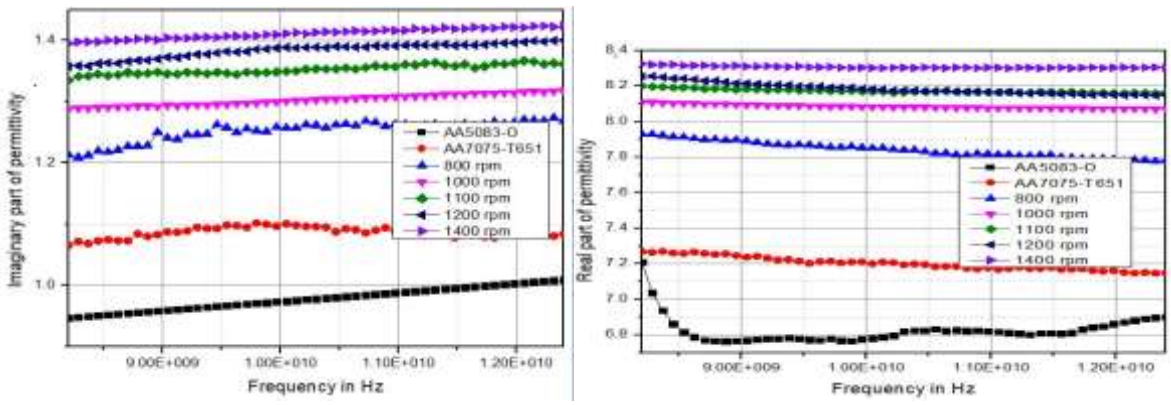

Fig.4 Imaginary and real permittivity of base alloys and FSW weld joints

Weld joint permittivity may have increased due to the development of porosity and the accumulation of conductive networks brought on by the formation of voids with an increase in tool rotating speed. Figure.5 depicts the complex permeability's real and imaginary parts. The permeability of the real part ranges from 0.8 to 1.2, whereas the permeability of the imagined part ranges from -0.3 to -0.9. Real permeability of weld joints and base alloys is higher than that of air (which is 1) and rises with increasing tool rotating speed while falling with frequency. Real permeability variation caused by the eddy current effect. Base alloy shielding efficiency is zero due to relatively high impedance mismatch in comparison to the weld joints. The presence of these features in weld joints may promote the creation of voids that scatter EMI signals because micro-voids find it harder to exit from porous media and micro voids.

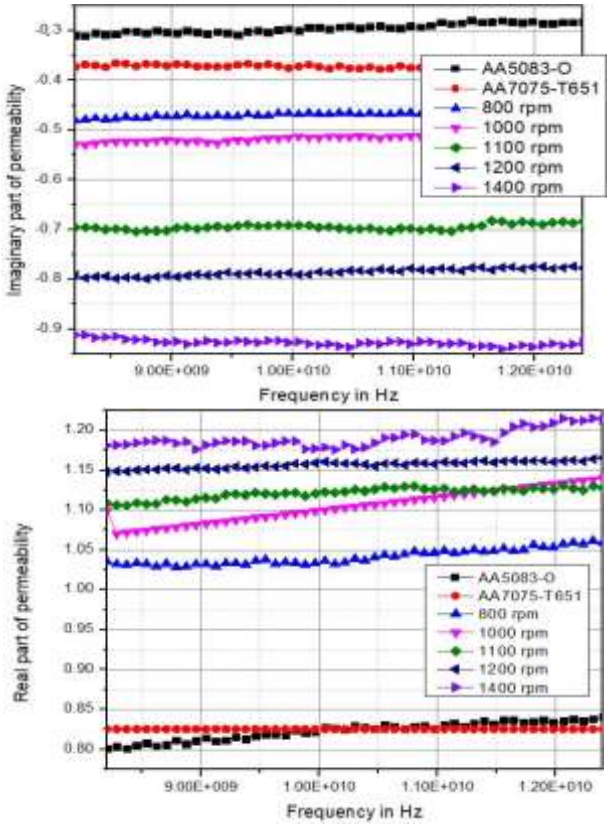

Fig.5 Imaginary and real permeability of base alloys and FSW weld joints

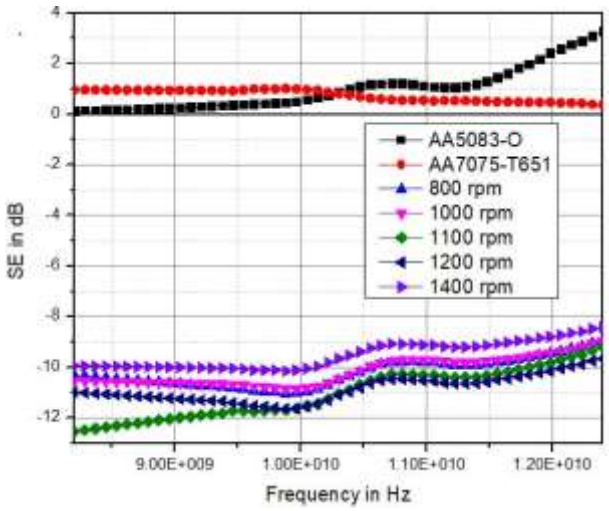

Fig.6 shielding effectiveness of base alloys and FSW weld joints

3.3 Corrosion of TIG weld joints

It is well recognised that corrosion can ruin a material's useful characteristics and make it unsuitable for its intended use. Weld joints constructed of different materials and exposed to the environment are very susceptible to corrosion. A considerable impact of alloying elements on the mechanical characteristics and corrosion resistance of aluminium. The propensity for corrosion is increased by elements like copper, silicon, and magnesium, whilst the resistance to corrosion is increased by addition. However, the alloying elements do have a limited degree of solid solubility in aluminium at specific temperatures and concentrations. Figure.7 shows the results of potentiodynamic polarization, and it is clear that the corrosion potential (Ecorr) varies from one weld sample to another. Compared to other amps, 80 amps have reduced corrosion resistance. It might be caused by the dissolution of strengthening phases and the creation of galvanic connection between the intermetallic and Al-matrix. In contrast to fine equiaxed (-712mVs), the presence of coarse grain improves intergranular corrosion resistance (-606.89mVs). In addition to providing high strength, the distribution of fine precipitates may also encourage galvanic coupling by lowering corrosion resistance as compared to 90 amps.

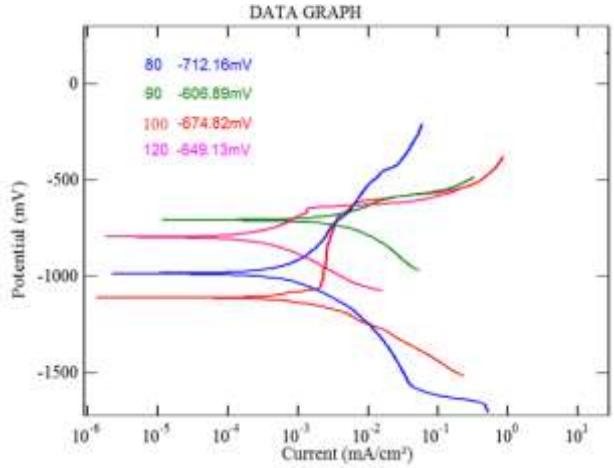

Fig.7 Potentiodynamic polarization curves of the weld joints

4.0 Conclusions

The current research demonstrates that TIG and FSW techniques can successfully join dissimilar AA5083-O and AA7075-T651 aluminium alloys. The investigation led to the following findings.

- Formation of intermetallics and precipitates resulted in superior joint line hardness for welds made at 120 amp current.
- Pitting corrosion characteristic of weld joints showed that corrosion resistance of weld made at 90 amps superior to other joints.
- EM wave properties like permeability and permeability significantly influenced by the weld current
- Shielding of all weld joints follows a similar trend in the entire frequency band.

References

1. Ch Hima Gireesh, Koona Ramji, K.G Durga Prasad, Budumuru Srinu(2019) Study of Mechanical Properties and EMI Shielding Behavior of Al6061 Hybrid Metal Matrix Composites, International Journal of Surface Engineering and Interdisciplinary Materials Science 7(2),48-63.
2. Xiangyu Ma, Qiang Zhang,, Zhichao Luo, Xiu Lin, GaohuiWu,(2016) A novel structure of Ferro-Aluminum based sandwich composite for magnetic and electromagnetic interference shielding,Materials and Design 89,71–77.
3. Zuwei Fan, Rangtong Liu and Xiaojie Cheng,(2021) Preparation and Characterization of Electromagnetic Shielding Composites Based on Graphene-Nanosheets-Loaded Nonwoven Fabric,Coatings,11, 424.
4. S. Geetha,K. K. Satheesh Kumar,Chepuri R. K. Rao,M. Vijayan,D. C. Trivedi,(2009) EMI shielding: Methods and materials—A review, Journal of Applied Polymer Science 112(4), 2073 - 2086.
5. M. K. Naidu, K. Ramji, B. V. S. R. N. Santhosi, TC Shami, Himangshu B Baskey, B. Satyanarayana, (2017) Enhanced Microwave Absorption of Quartic Layered Epoxy-Mwcnt Composite for Radar Applications, Composites and Advanced Materials, https://doi.org/10.1177/096369351702600405.
6. Avinash R. Pai, Nizam Puthiyaveettil Azeez,Binumol Thankachan,Nandakumar Gopakumar, Maciej Jaroszewski, Claudio Paoloni, Nandakumar Kalarikkal and Sabu Thomas,(2022) Recent Progress in Electromagnetic Interference Shielding Performance of Porous Polymer Nanocomposites—A Review, Energies 15(11), 3901.
7. Jeevan Kittur, Bhavya Desai, Rakesh Chaudhari, Praveen Kumar Loharkar, (2020) A comparative study of EMI shielding effectiveness of metals,metal coatings and

carbon-based materials,IOP Conf. Series: Materials Science and Engineering 810, 012-019.

8. Srinu Budumuru,M. Satya Anuradha,(2021) Electromagnetic shielding and mechanical properties of AL6061 metal matrix composite at X‑ band for oblique incidence,Advanced Composites and Hybrid Materials 4,1113–1121.
9. Do Z, Wu G, Huang X, Sun D, & Jiang L,(2007) Electromagnetic shielding effectiveness of aluminum alloy-fly ash composites. Composites. Part A, Applied Science and Manufacturing, 38(1), 186–191.
10. Zuoyong Dou,Gaohui Wu,Xiaoli Huang, Dongli Sun, Longtao Jiang,Electromagnetic shielding effectiveness of aluminum alloy–fly ash composites,Composites: Part A 38 (2007) 186–191.
11. Yao W lin, Xiong G, Yang Y, Huang H qing and Zhou Y fen 2017 Effect of silica fume and colloidal graphite additions on the EMI shielding effectiveness of nickel fiber cement based composites Constr. Build. Mater. 150 825–32
12. D. Bacioiv, G. Melton, M. Papaelias, R. Shaw. Automated defect classification of Aluminium 5083 TIG welding using HDR camera and neural networks: Journal of Manufacturing Process 2019; 45:603-613.
13. A.Kumar, S. Sundarrajan. Optimization of pulsed TIG welding process parameters on mechanical properties of AA 5456 Aluminium alloy weldments. Materials & Design 2009;30(4) :1288-1297.
14. Y. Liang, J.Q. Shen, S.S. Hu, H.C. Wang, J. Pang. Effect of TIG current on microstructural and mechanical properties of 6061-T6 aluminium alloy joints by TIG-CMT hybrid welding: Journal of Material Process Technology 2018; 255:161-174.
15. Liamine Kaba,Mohammed Elamine Djeghlal, Seddik Ouallam & Sami Kahla,Dissimilar welding of aluminum alloys 2024 T3 and 7075 T6 by TIG process with double tungsten electrodes,The International Journal of Advanced Manufacturing Technology,2022, 118, 937–948.
16. Z. Y. Ma, A. H. Feng, D. L. Chen, and J. Shen, Recent Advances in Friction Stir Welding/Processing of Aluminum Alloys:Microstructural Evolution and Mechanical Properties, critical reviews in solid state and materials sciences,2017,0,1-65
17. Ilangovan M, Boopathy SR, Balasubramanian V, Effect of tool pin profile on microstructure and tensile properties of friction stir welded dissimilar AA 6061–AA 5086 aluminum alloy joints. Defence Technology, 2015, 11,174–184.
18. P.L. Threadgill, A.J. Leonard, H.R. Shercliff, and P.J. Withers, Friction Stir Welding of Aluminium Alloys, International Material Reviews, 2009, 54(2), 49–93

19. R. Palanivel, P. Koshy Mathews,N. Murugan, I. Dinaharan,Effect of tool rotational speed and pin profile on microstructure and tensile strength of dissimilar friction stir welded AA5083-H111 and AA6351-T6 aluminum alloys, Materials and Design 2012,40, 7–16.
20. Kasman S, Yenier Z,Analyzing dissimilar friction stir welding of AA5754/AA7075. International Journal of Advanced Manufacturing Technology, 2014, 70, 145– 156.
21. Sivachidambaram S, Rajamurugan G, Amirtharaj D, Optimizing the parameters for friction stir welding of dissimilar aluminium alloys AA5383/AA7075. ARPN Journal of Engineering and Applied Sciences, 2015, 10,5434–5437
22. Waseem S Abbas, Muhaed Alali , Salim J (2021) 'Effect of rotational speed and tool pin profile on the corrosion rate of friction stir welded AA6061-T3' IOP Conf. Series: Materials Science and Engineering, 1090
23. Chandrasekaran Shyamlal, Rajesh Shanmugavel , J. T. Winowlin Jappes, Anish Nair, M. Ravichandran , S. Syath Abuthakeer , Chander Prakash , Saurav Dixit and N. I. Vatin (2022) 'Corrosion Behavior of Friction Stir Welded AA8090-T87 Aluminum Alloy' Materials,15,51-65
24. R.W. Fonda, P.S. Pao, H.N. Jones, C.R. Feng,B.J. Connolly, A.J. Davenport (2009) 'Microstructure, mechanical properties, and corrosion of friction stir welded Al 5456' Materials Science and Engineering A, 519, 1–8
25. Guidelines for Limiting Exposure to Electromagnetic Fields (100 kHz to 300 GHz), International Commission on Non-Ionizing Radiation Protection (ICNIRP). Health Phys. 2020, 118, 483–524.
26. B V S R N Santhosi,K Ramji,N B R Mohan Rao and M K Naidu. Comparative study of polymer-based nanocomposites microwave absorption performance in X–band. Materials Research Express, 2020, 7(1), DOI:10.1088/2053-1591/ab621e